

RAPID COMMUNICATIONS

Uroguanylin and Guanylin: Distinct But Overlapping Patterns of Messenger RNA Expression in Mouse Intestine

TERESA L. WHITAKER,* DAVID P. WITTE,† M. CATHERINE SCOTT,* and MITCHELL B. COHEN*

Divisions of *Pediatric Gastroenterology and Nutrition and †Pediatric Pathology, Children's Hospital Medical Center, University of Cincinnati, Cincinnati, Ohio

See editorial on page 1036.

Background & Aims: Uroguanylin and guanylin, endogenous ligands of the guanylate cyclase C receptor, are presumed to mediate fluid and electrolyte secretion in the intestine. The aim of this study was to characterize the expression patterns of uroguanylin and guanylin messenger RNA (mRNA) in the mouse intestine. **Methods:** A mouse uroguanylin complementary DNA was amplified from a partial genomic clone, and Northern analyses and in situ hybridization were performed to localize guanylin and uroguanylin mRNA along the duodenal-colonic and crypt-villus axes. **Results:** Uroguanylin mRNA was expressed throughout the mouse intestine and also in the kidney. Signal intensity was greatest in the small intestine for uroguanylin and in the distal small intestine and colon for guanylin. In situ hybridization showed uroguanylin mRNA localized predominantly in intestinal villi and the corticomedullary junction of the kidney, whereas guanylin mRNA was localized in both crypts and villi in the small intestine and to superficial epithelial cells in the colon. **Conclusions:** Mouse uroguanylin mRNA expression is discrete from guanylin expression in the intestine. The patterns of distribution in the intestine and the known pH optima of these ligands suggest a complementary role for these secretagogues.

Heat-stable enterotoxin (STa) is a peptide ligand elaborated by *Escherichia coli* and other bacteria.¹ Binding of this ligand to the intestinal receptor guanylate cyclase C (GC-C) results in increased intracellular levels of guanosine 3',5'-cyclic monophosphate (cGMP).² This, in turn, activates a cGMP-dependent protein kinase (cGKII),³ which phosphorylates the cystic fibrosis transmembrane conductance regulator (CFTR), resulting in net chloride (Cl⁻) and water secretion.^{4,5} Infection with STa-producing *E. coli* results in secretory diarrhea.¹ Two endogenous ligands, guanylin and uroguanylin, which

transduction pathway, causing net Cl⁻ secretion.⁴⁻⁷ However, guanylin and uroguanylin are less potent activators of GC-C than STa.^{6,8,9} Guanylin and STa have also been shown to stimulate duodenal bicarbonate (HCO₃⁻) secretion.¹⁰

Guanylin was originally isolated from the rat jejunum.⁷ Although uroguanylin was originally identified in opossum and human urine,^{6,9} similar to guanylin, uroguanylin messenger RNA (mRNA) is predominantly expressed in the intestine.^{11,12} However, the precise location of uroguanylin mRNA in the intestine, along the longitudinal (duodenal-colonic) and crypt-villus axes, has been less well studied.¹¹ Uroguanylin mRNA expression has also been reported in opossum kidney and heart¹³ and in rat lung, pancreas, and kidney.¹¹

To determine the functions of these endogenous ligands within the intestine, it is important to localize their sites of expression. In this study, we describe cloning of the mouse uroguanylin complementary DNA (cDNA) and characterization of the tissue and cellular location of uroguanylin and guanylin mRNA in the mouse. We show a distinct, yet overlapping pattern of expression for guanylin and uroguanylin in the mouse intestine as well as extraintestinal expression of uroguanylin in the kidney.

Materials and Methods

cDNA Cloning

A single 4-kilobase (kb) *Xba*I-*Xba*I fragment from a genomic clone (accession no. U95182) was subcloned into pBluescript II SK⁺ (Stratagene, La Jolla, CA). Overlapping oligonucleotide primers were used to sequence the ends until sequences homologous to the human uroguanylin cDNA¹⁴

Abbreviations used in this paper: CFTR, cystic fibrosis transmembrane conductance regulator; cGKII, guanosine 3',5'-cyclic monophosphate-dependent protein kinase II; GC-C, guanylate cyclase C; RT-PCR, reverse-transcription polymerase chain reaction; STa, heat-stable enterotoxin.

© 1997 by the American Gastroenterological Association

were observed. Two polymerase chain reaction (PCR) primers were then designed for the cDNA ends (5' primer, AGGTGG-ACAGCAGAAGGAAG; 3' primer, TGGTGCCTAAGT-ATGGAC) and used to amplify a partial 450-nucleotide cDNA from strain FVB/NJ mouse intestinal total RNA using reverse-transcription (RT)-PCR as described previously.¹⁵ Sequencing confirmed the fidelity of the fragment subcloned into PCR 2.1 (Invitrogen, Carlsbad, CA). Sequences were analyzed using MacVector sequence analysis software (Eastman Kodak, Rochester, NY).

Northern Blot Analysis

Total RNA was isolated from a panel of strain FVB/NJ mouse tissues using acid guanidine isothiocyanate-phenol-chloroform extraction.¹⁶ Mouse tissues were harvested under a protocol approved by the Institutional Animal Care and Use Committee. For intestinal tissues, segments were divided into the following: duodenum (first 3 cm distal to stomach), proximal jejunum (proximal one third of small intestine), distal jejunum (central one third of small intestine), ileum (distal one third of small intestine), cecum, proximal colon (proximal two fifths of large intestine), and distal colon (distal three fifths of large intestine). Total RNA (20 µg) was electrophoresed through a 1.0% agarose/1.9% formaldehyde denaturing gel, transferred to a nylon membrane (MagnaGraph; MSI, Westborough, MA), and cross-linked to the membrane using UV light (Stratalinker; Stratagene) as described previously.¹⁷ Blots were hybridized with cDNA fragments generated by PCR encompassing nucleotides 288–386 of mouse uroguanylin and nucleotides 118–307 of mouse guanylin.¹⁸ Each PCR product was subcloned into PCR 2.1, and the resultant plasmids were called PCR 2.1 m.uro 98 and PCR 2.1 m.gg exon 2. An end-labeled oligonucleotide complementary to 18S ribosomal RNA was used for quantitation of relative amounts of total RNA loaded and normalization of signal intensities.¹⁹ Northern blots were hybridized overnight at 60°C and were washed under high-stringency conditions as described previously.¹⁹ Image analysis and mRNA quantitation were performed on a surface emission scanner (Molecular Dynamics PhosphorImager; Molecular Dynamics, Sunnyvale, CA) using ImageQuant software (Molecular Dynamics).

In Situ Hybridization

Tissues were processed for in situ hybridization as described previously.^{20,21} Briefly, fresh tissue was fixed in 4% paraformaldehyde and then saturated in 30% sucrose before being embedded in M1 embedding matrix (Lipshaw, Pittsburgh, PA) and snap-frozen. Cryostat sections were cut at 10–12 µm, air-dried on slides coated by Vectabond (Vector Laboratories, Burlingame, CA), and fixed with paraformaldehyde. Prehybridization and hybridization were performed as described previously.^{20,21} [³⁵S]uridine 5' triphosphate-labeled sense and antisense riboprobes were prepared from linearized PCR 2.1 m.uro 98 and PCR 2.1 m.gg exon 2 plasmids (described above). Tissue sections were photographed under dark-

A

```

GGGCTGCTGG CCCAAAAGGA GGGTGGCAGG CAGGTGGACA GCAGAGGAAG CAGGAACCCA 60
GAGGTGTGAG CTTGGAAGCA GGGGCCATGT CAAGAAGCCA ACTGTGGGCT GCCGTGCTCC 120
TGCTGCTGCT CCTGCGAAGT GCACAGGGTG TCTACATCAA GTACCATGGC TTCCAAGTCC 180
AGCTGGAATC AGTGAAGAAG CTGAATGAGT TGGAGGAGAA GGAGATGTCC AATCCCACAGC 240
CTGGGAGAAG TGGCCTCCTC CCTGCTGTGT GCCATAACCC AGCCTTGCCC TTGGACCTCC 300
AGCCTGTTTG TGCCCTCCAG GAAGCTGCCA GCACCTTCAA GGCCTTGAGG ACCATCGCCA 360
CCGACGAATG TGAACGTGTG ATAAATGTTG CCTGTACAGG CTGCTGATGA AATGACTCTG 420
GGCTTTAAGA CCACTCCGGA CACTTTCCCC ACAGCCCAAC CTGTCCATAC TTAGGCACCA 480
TTGAAGTAAT CGCCATCCTC CCAGCATAAA TGGATCCTTA GCAAGGCAAT GTGGATGCGA 540
AGTTGCCATA TTTGGCCCCC AGGCAGCTGC ACCTGAATAA AAAA 584

```

B

```

Met Ser Arg Ser Gln Leu Trp Ala Ala Val Val Leu Leu Leu Leu Arg Ser Ala Gln Gly
Val Tyr Ile Lys Tyr His Gly Phe Gln Val Gln Leu Glu Ser Val Lys Lys Leu Asn Glu
Leu Glu Glu Lys Glu Met Ser Asn Pro Gln Pro Arg Arg Ser Gly Leu Leu Pro Ala Val
Cys His Asn Pro Ala Leu Pro Leu Asp Leu Gln Pro Val Cys Ala Ser Gln Glu Ala Ala
Ser Thr Phe Lys Ala Leu Arg Thr Ile Ala Thr Asp Glu Cys Glu Leu Cys Ile Asn
Val Ala Cys Thr Gly Cys

```

Figure 1. (A) Sequence of mouse uroguanylin cDNA. The start site and the stop codon are underlined. The poly(A)⁺ signal is double-underlined. (B) Deduced amino acid sequence of mouse uroguanylin cDNA. The sequence of the 15 amino acid mature peptide is highlighted (---).

Results

Cloning of Mouse Uroguanylin cDNA

A single 4-kb genomic fragment was identified, which strongly hybridized with a ³²P-labeled human uroguanylin cDNA probe (gift of O. Hill¹⁴). This fragment was subcloned into pBluescript II SK⁺ and further analyzed by restriction mapping and direct dideoxynucleotide sequencing. We were able to identify the 5' and 3' ends of the coding sequence from the sequence information. Using primers designed for each, we used RT-PCR to amplify 450 nucleotides of mouse uroguanylin cDNA from total RNA extracted from mouse jejunum. This amplified product was then subcloned into the PCR 2.1 vector. From direct sequencing of the genomic fragment, we predicted the cDNA start site near a TATAA sequence upstream of the coding sequence. The location of the poly(A)⁺ signal sequence predicted a full-length cDNA of 590 nucleotides.

The sequence of the full-length mouse uroguanylin cDNA (accession no. U90727) and the predicted amino acid sequence are shown in Figure 1. The mouse uroguanylin cDNA shares 82% homology with human uroguanylin,¹⁴ 90% homology with rat uroguanylin,¹¹ and 51% homology with mouse guanylin.¹⁸ In addition, the uroguanylin cDNA is 99% identical to an unpublished expressed sequence tag cloned from mouse kidney.²² Translation of the mouse uroguanylin cDNA predicts a 106–

of the mature carboxy-terminal 15–amino acid peptide is 80% identical to the predicted human sequence¹⁴ and 93% identical to the rat peptide.¹¹

Northern Analysis

A 98–base pair (bp) fragment extending from nucleotides 288–386 was used as a probe for Northern blot analysis to localize mouse uroguanylin mRNA. A single predominant mRNA species of approximately 600 bp was recognized with this probe. Signal was present in all intestinal tissues examined, with highest concentrations observed in the duodenum, jejunum, and ileum (Figure 2). Extraintestinal expression was also found in the kidney (Figure 2). No signal was detected in the liver, spleen, heart, lung, brain (Figure 2), stomach, or thymus (not shown). As shown in Figure 2, this expression pattern is distinct from that observed when the same blot was probed with a guanylin cDNA; guanylin message was also present in all intestinal tissues but was most prevalent in the distal jejunum, ileum, cecum, and colon; no extraintestinal expression of guanylin was found by Northern analysis. Quantitation of relative signal intensities for both uroguanylin and guanylin is shown in Figure 3.

In Situ Hybridization

To further delineate the crypt-villous and extraintestinal expression pattern of mouse uroguanylin and

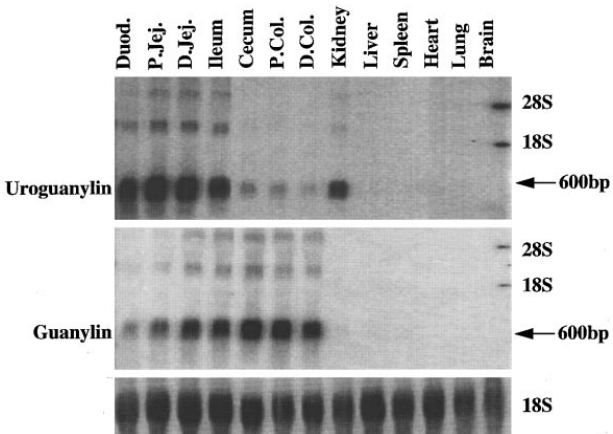


Figure 2. Representative Northern analysis of guanylin and uroguanylin message. Total RNA was separated and the blot was probed as described in Materials and Methods. The positions of 28S and 18S rRNA are indicated along the side of each blot. Both guanylin and uroguanylin mRNA were present throughout the intestine. Unlike guanylin mRNA, which was highest in distal small intestine and colon, uroguanylin signal was highest in small intestine with very little signal in the cecum and colon. Uroguanylin signal was also found in the kidney but not in liver, spleen, heart, lung, or brain. No extraintestinal expression of guanylin was detected. For quantitation purposes, the blot was reprobed with an oligonucleotide that recognizes 18S rRNA¹⁹.

guanylin, we performed in situ hybridization of a panel of mouse tissues using ³⁵S-labeled sense and antisense riboprobes. Both antisense probes showed highly restricted patterns of expression. In the duodenum, uroguanylin signal was primarily in midvillous epithelial cells (Figure 4A, arrow). Signal in isolated crypt cells (arrowheads) was detected by dark-field illumination with both sense (Figure 4B) and antisense probes (Figure 4A) and is caused by autofluorescence of Paneth cell granules.²³ Absence of bona fide signal was confirmed by bright-field microscopy (data not shown). Intense uroguanylin signal in the proximal jejunum was primarily seen in villous epithelium, although a uniform narrow band of autoradiographic grains was also present at the base of the crypts (Figure 4C). In distal jejunum and ileum, the uroguanylin signal appeared to be restricted to villous epithelium (Figure 4D–F). As with the duodenal crypt cell expression, the signal in isolated crypt cells in distal jejunum and ileum results from Paneth cell autofluorescence rather than autoradiographic grains (Figure 4D and E). At the ileocecal boundary, uroguanylin signal was only detected in epithelial cells overlying a lymphoid aggregate (Figure 4F, arrow). No uroguanylin signal was detected in the colon (Figure 4G), raising the possibility that the level of expression of uroguanylin mRNA in the colon is below the level of detection of our in situ

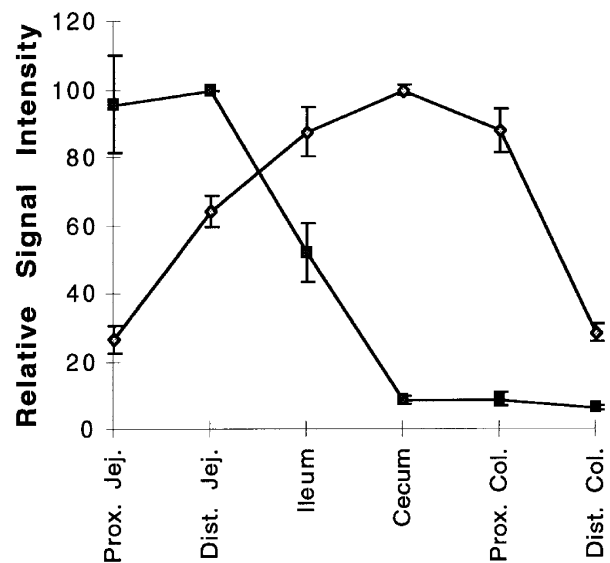


Figure 3. Quantitation of relative signal intensities for guanylin (◆) and uroguanylin (■) mRNA in mouse intestine. All quantitation was performed with ImageQuant software. Relative signal intensities were normalized to 18S ribosomal RNA signal intensity.¹⁹ Guanylin values are shown as a percentage of cecum signal intensity with cecum set at 100%. Uroguanylin values are shown as a percentage of proximal jejunal expression with this value set at 100%. Data are mean ± SE.

hybridization experiments or that the signal found by Northern analysis represents weak cross-hybridization with guanylin mRNA. We also found a discrete band of uroguanylin message in the kidney, in cells localized to the corticomedullary junction (Figure 4H), using the antisense probe; no signal was seen with the sense probe (Figure 4I).

In contrast to uroguanylin, authentic and robust guanylin message was detected in crypt cells in the proximal and distal jejunum and ileum (Figure 4J, L, and M). Guanylin mRNA was also present in many but not all villous cells in the proximal jejunum (Figure 4J) and in all villous cells in the distal jejunum (Figure 4L) and ileum (Figure 4M). The most intense signal was observed in the superficial epithelium of the cecum and colon (Figures 4N, O, and P). Interestingly, guanylin mRNA was limited to the superficial epithelium in distal colon (Figure 4P) but was present in the neck and deeper colonic glands in proximal colon (Figure 4O). The broader distribution of signal in proximal than in distal colon correlated with the increased expression detected by Northern analysis (Figures 2 and 3). No signal was seen using the sense probe in proximal jejunum (Figure 4K) and colon (Figure 4Q). No guanylin signal was detected in mouse kidney (data not shown).

Discussion

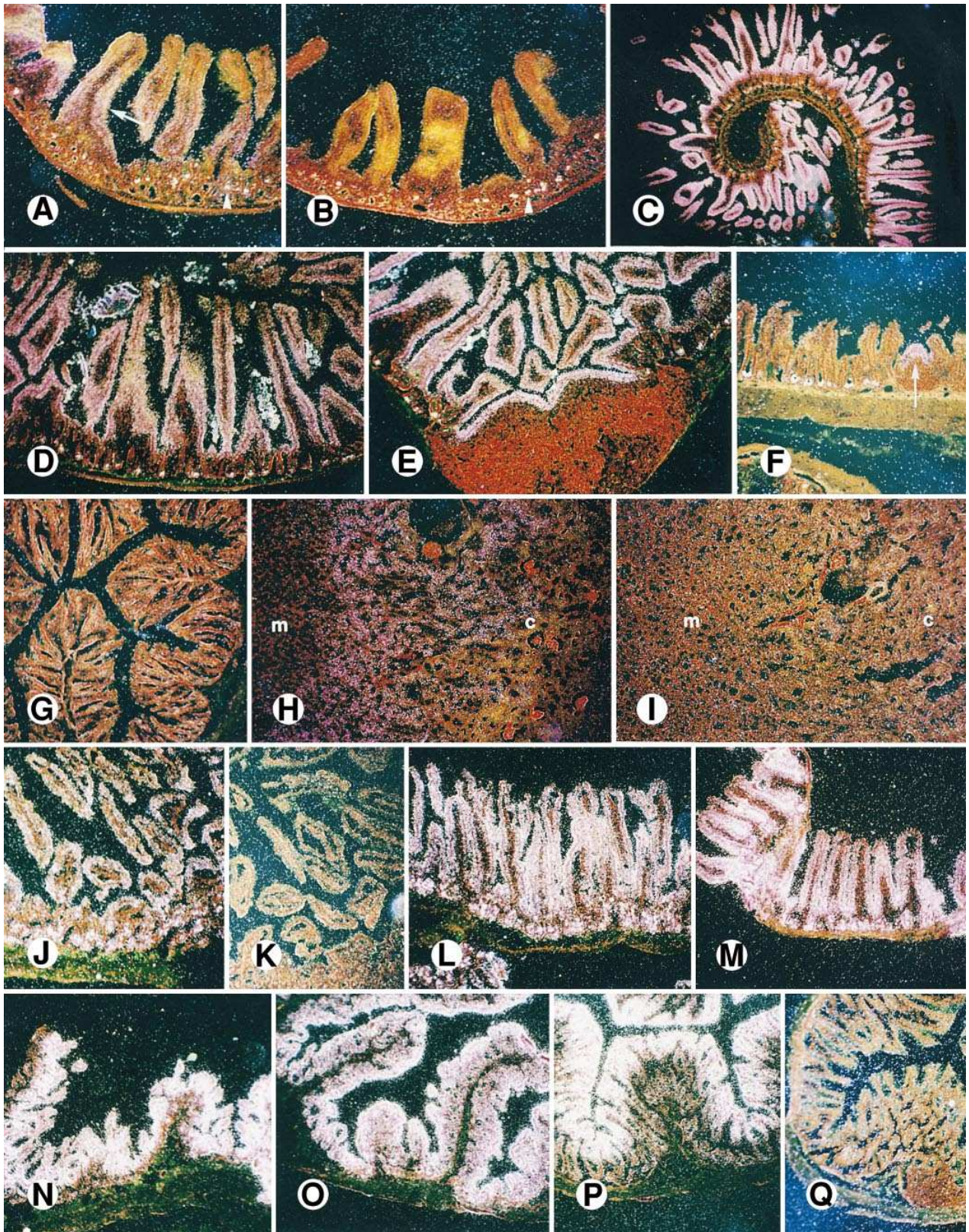
We have cloned a mouse uroguanylin cDNA and showed a discrete yet overlapping pattern of expression for mouse uroguanylin and guanylin. Although guanylin and uroguanylin mRNA are found throughout the mouse intestine, their levels of expression vary in different segments, and they seem to be expressed by different cell types. The highest level of uroguanylin mRNA expression occurs in the proximal small intestine; the highest level of guanylin mRNA expression occurs in the distal small intestine, cecum, and proximal colon. Mouse uroguanylin mRNA is primarily restricted to the villi, whereas guanylin mRNA is localized to both crypts and villi throughout the small intestine.

Our observations are consistent with the reported distribution of uroguanylin mRNA in rat intestine and kidney,¹¹ although the tissue-specific pattern of uroguanylin mRNA expression in the mouse is more restricted than previously reported for rats¹¹ and opossums.¹³ Uroguanylin mRNA was found in human colon; no signal was found in the kidney, and the small intestine was not investigated.¹⁴ The cellular localization of uroguanylin has not been previously reported for any species.^{11,13,14} We have also shown that guanylin mRNA is expressed throughout the mouse intestine, as has been shown in

both crypt and villous cells in the mouse intestine correlates with the distribution of guanylin mRNA we have observed in human intestine²⁵ but not with the villous pattern we observed in the rat.²¹ This species-specific pattern of guanylin mRNA expression parallels the pattern of GC-C mRNA expression, which is primarily restricted to villous cells in the rat small intestine¹⁹ but includes both crypt and villous epithelium in the mouse.²⁶

On the basis of the localization data in this study for guanylin and uroguanylin mRNA and previously documented distribution patterns for GC-C,²⁶ CFTR,²⁷ and cGKII,²⁸ the entire guanylin/uroguanylin-mediated signal transduction pathway is probably localized to some of the same epithelial cells. Mouse GC-C mRNA is expressed in both crypts and villi in the small intestine and in the deep crypts and superficial epithelium of the large intestine.²⁶ cGKII mRNA expression has not been examined in mice, but in rats, cGKII mRNA expression extends from the crypts to the upper villous, with the highest level of expression in midvillous cells in the small intestine. Expression of cGKII mRNA is also found in the crypts of the cecum and proximal colon²⁸; no cGKII expression is found in the distal colon.²⁸ Mouse CFTR mRNA is present in the small intestine and colon. In the small intestine, it is predominantly expressed in the crypts with a decreasing gradient along the villi, with no expression at the villous tips.²⁷ Thus, in the small intestine, there is probably colocalization of guanylin and/or uroguanylin, GC-C, cGKII, and CFTR mRNA within the same cells in the crypts and bottom one third of the villi. The entire secretory pathway is also likely to be present in guanylin mRNA-expressing cells in the cecum and proximal colon. The observation of uroguanylin mRNA expression in epithelial cells overlying lymphoid aggregates parallels the distinctive pattern of CFTR mRNA expression in epithelial cells in close contact with lymphoid tissue in human intestine.²⁹ However, guanylin, uroguanylin, and GC-C mRNA are also present in high concentrations in villous cells where CFTR is poorly or not at all expressed,^{26,27} and guanylin and GC-C are present in the distal colon where cGKII may not be expressed.²⁸ Therefore, it is possible that there are other downstream targets or intermediaries of this endogenous receptor-ligand interaction.

Guanylin and uroguanylin have different pH optima of activity, with uroguanylin functional at pH ~5.5 and guanylin at pH ~8.0.³⁰ Also, a pH microclimate exists along the villi of the jejunum; in rats, the pH gradient changes from pH 6.6 at the villous tip to pH 8.15 in the crypts³¹; it is likely that a similar microclimate exists



MSN Exhibit 1051 - Page 5 of 7

Explore Litigation Insights

Docket Alarm provides insights to develop a more informed litigation strategy and the peace of mind of knowing you're on top of things.

Real-Time Litigation Alerts



Keep your litigation team up-to-date with **real-time alerts** and advanced team management tools built for the enterprise, all while greatly reducing PACER spend.

Our comprehensive service means we can handle Federal, State, and Administrative courts across the country.

Advanced Docket Research



With over 230 million records, Docket Alarm's cloud-native docket research platform finds what other services can't. Coverage includes Federal, State, plus PTAB, TTAB, ITC and NLRB decisions, all in one place.

Identify arguments that have been successful in the past with full text, pinpoint searching. Link to case law cited within any court document via Fastcase.

Analytics At Your Fingertips



Learn what happened the last time a particular judge, opposing counsel or company faced cases similar to yours.

Advanced out-of-the-box PTAB and TTAB analytics are always at your fingertips.

API

Docket Alarm offers a powerful API (application programming interface) to developers that want to integrate case filings into their apps.

LAW FIRMS

Build custom dashboards for your attorneys and clients with live data direct from the court.

Automate many repetitive legal tasks like conflict checks, document management, and marketing.

FINANCIAL INSTITUTIONS

Litigation and bankruptcy checks for companies and debtors.

E-DISCOVERY AND LEGAL VENDORS

Sync your system to PACER to automate legal marketing.